AD-A183 356 THE INFLUENCE OF DESORPTION KINETICS ON HYDROGEN PERMEATION IN IRON(U) RENSSELAER POLYTECHNIC INST TROY NY DEPT OF MATERIALS ENGINEERING M ARBAB ET AL. 1/1

UNCLASSIFIED 30 JUL 87 TR-1 N00014-86-K-0259 F/G 7/4 NL

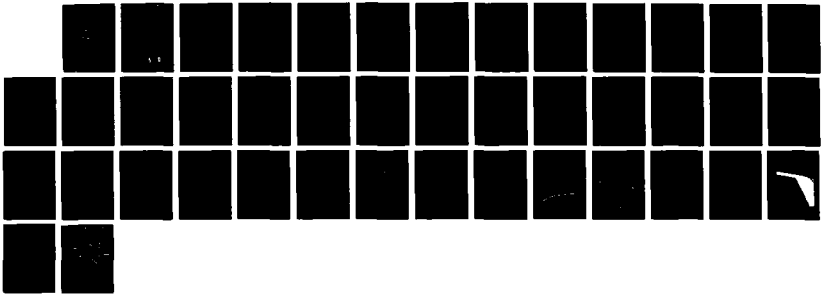

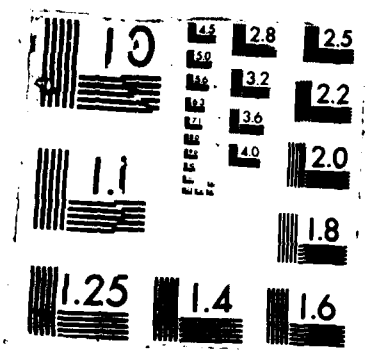
1.0
1.1
1.25
1.4
1.6
1.8
2.0
2.2
2.5
2.8
3.2
3.6
4.0
4.5
5.0

DTIC FILE COPY (12)

Unclassif
SECURITY CLASSI

UMENTATION PAGE

AD-A183 356

1a. REPORT SECU Uncl...	1b RESTRICTIVE MARKINGS
2a. SECURITY CLASSIFICATION AUTHORITY	3 DISTRIBUTION / AVAILABILITY OF REPORT Approved for public release; distribution unlimited
2b. DECLASSIFICATION / DOWNGRADING SCHEDULE	
4. PERFORMING ORGANIZATION REPORT NUMBER(S) Technical Report #1	5. MONITORING ORGANIZATION REPORT NUMBER(S)
6a. NAME OF PERFORMING ORGANIZATION Materials Engineering Dept. RPI	6b. OFFICE SYMBOL (If applicable)
6c. ADDRESS (City, State, and ZIP Code) Troy, NY 12180-3590	7a. NAME OF MONITORING ORGANIZATION Office of Naval Research
	7b. ADDRESS (City, State, and ZIP Code) Chemistry Program 800 N. Quincy Street Arlington, VA 22217
8a. NAME OF FUNDING / SPONSORING ORGANIZATION Office of Naval Research	8b. OFFICE SYMBOL (If applicable)
	9. PROCUREMENT INSTRUMENT IDENTIFICATION NUMBER Contract # N00014-86-K-0259
8c. ADDRESS (City, State, and ZIP Code) Chemistry Program 800 N. Quincy St. Arlington, VA 22217	10 SOURCE OF FUNDING NUMBERS PROGRAM ELEMENT NO. / PROJECT NO. / TASK NO. / WORK UNIT ACCESSION NO

11. TITLE (Include Security Classification)
"The Influence of Desorption Kinetics on Hydrogen Permeation in Iron"

12. PERSONAL AUTHOR(S)
M. Arbab and J. B. Hudson

13a. TYPE OF REPORT	13b. TIME COVERED	14. DATE OF REPORT (Year, Month, Day)	15. PAGE COUNT
Interim Technical	FROM _____ TO _____	1987-7-30	38

16. SUPPLEMENTARY NOTATION
To be published in Applied Surface Science

17 COSATI CODES			18. SUBJECT TERMS (Continue on reverse if necessary and identify by block number)
FIELD	GROUP	SUB-GROUP	

19. ABSTRACT (Continue on reverse if necessary and identify by block number)

The common observation that the diffusivity of hydrogen in iron decreases anomalously at low temperatures is treated in terms of the barrier to adatom recombination and desorption that is known to be associated with the surfaces of this metal. Results obtained are in good agreement with both data on deuterium permeation through a polycrystalline iron sample, obtained in this study, and with the body of measurements for hydrogen diffusion through iron found in the literature.

20 DISTRIBUTION / AVAILABILITY OF ABSTRACT	21 ABSTRACT SECURITY CLASSIFICATION
☒ UNCLASSIFIED/UNLIMITED ☒ SAME AS RPT ☐ DTIC USERS	Unclassified
22a NAME OF RESPONSIBLE INDIVIDUAL Dr. David L. Nelson	22b TELEPHONE (Include Area Code) (202) 696-4410
	22c OFFICE SYMBOL

DD FORM 1473, 84 MAR 83 APR edition may be used until exhausted. All other editions are obsolete

SECURITY CLASSIFICATION OF THIS PAGE

87 8 14 014

OFFICE OF NAVAL RESEARCH

Contract N00014-86-K-0259

Task No. NR-056-533

TECHNICAL REPORT NO. 1

THE INFLUENCE OF DESPORTION KINETICS ON HYDROGEN PERMEATION IN IRON

by

M. Arbab and J. B. Hudson

Rensselaer Polytechnic Institute
Materials Engineering Department
Troy, New York 12180-3590

July 30, 1987

Abstract

The common observation that the diffusivity of hydrogen in iron decreases anomalously at low temperatures is treated in terms of the barrier to adatom recombination and desorption that is known to be associated with the surfaces of this metal. Results obtained are in good agreement both with data on deuterium permeation through a polycrystalline iron sample, obtained in this study, and with the body of measurements for hydrogen diffusion through iron found in the literature.

1. Introduction

The interaction of hydrogen with iron has significant effects on the mechanical behavior of ferrous alloys and has motivated numerous experimental and theoretical studies. Many investigations concerning the thermal transport of hydrogen in iron have been carried out, and have shown a wide scatter in the magnitude of apparent interstitial diffusivities. In addition, a nonconformity to the Arrhenius behavior is observed for temperatures lower than 200°C [1].

Different hydrogen interstitial-trap interactions have been considered in order to explain the observed anomalies. These traps include such lattice defects as solid-solid interfaces (e.g. inclusions and microcracks) [2], substitutional and interstitial impurities [3,4], and line defects [16]. Furthermore, the formation of hydrogen di-interstitials in equilibrium with hydrogen single interstitials (the mobile species) [5], as well as hydrogen precipitation in voids [19], have been proposed to explain the deviation from the logarithmic behavior at low temperatures.

On the other hand, Volkl and Alefeld [1] and Kiuchi and McLellan [6], in their respective reviews of the experimental results, have argued that the anomalies should be explained in terms of surface effects, in those cases where surface processes are involved in the experimental methods employed (e.g. permeation methods). Also, in an electrochemical study of hydrogen permeation in iron, Wach and Miodownik [17] observed

that the apparent diffusivity of hydrogen at 25°C increased rapidly with membrane thickness and approached an upper limit. Such effects have been generally associated with the presence of oxides and impurities on the sample surface [6]. Indeed, the presence of an oxide film has been shown to decrease the apparent diffusivity of hydrogen in iron [7].

No study of the effects of the intrinsic properties of an atomically clean surface on the permeation behavior has been performed heretofore. Miller et al. [8] and Quick and Johnson [11] studied hydrogen permeation in high purity and 4-pass zone refined iron samples which were coated with a thin film of palladium. They reported no deviation from Arrhenius behavior for temperatures as low as 69°C and 49°C, respectively. In contrast, Nelson and Stein [9] observed such a deviation for their triply zone refined iron samples below 75°C. Their standard metallographic surface cleaning procedure however, could not have resulted in an atomically clean surface.

It was, therefore, the aim of this study to examine the effect of a clean and well annealed surface on the permeation of hydrogen in iron as a function of temperature. We report the results of a set of experiments, and will subsequently consider the surface effects, based on known desorption kinetics, to explain the low temperature anomalies.

2. Experimental

2.1 Apparatus

An all stainless steel ultrahigh vacuum system comprised of two chambers was employed in this study (Fig. 1a). The chambers were interconnected through a 1.45 mm diameter orifice. The main chamber was equipped with a 200 liter/second ion pump and a titanium sublimation pump, an Auger electron spectrometer (AES), an ion gun for sputter cleaning of the sample surface, an ionization gauge, and the sample manipulator. A base pressure of 5×10^{-10} torr could be attained after bake out.

The detector chamber housed a quadrupole mass spectrometer (QMS) and was evacuated by a closed cycle helium refrigerator cryopump to a base pressure of better than 2×10^{-10} torr (ionization gauge limit).

During a typical high temperature permeation experiment at 500°C, the total pressure of the main chamber rose to 1×10^{-7} torr. This pressure increase did not noticeably affect the detector chamber ion gauge reading.

The permeation cell is shown schematically in Figure 1b. It was constructed from a low carbon steel. The high purity, 1 mm thick iron sample (Marz Grade, Material Research Corporation) was TIG welded to the cell. A tantalum filament, located in the back of the permeation cell, was used to heat the sample by electron bombardment. Sample temperature was monitored by a W-5%Re, W-26%Re thermocouple spot welded near the front of the cell. The inner volume of the cell was pumped by a mechanical pump which was valved off during the permeation experiments. The inner surface of the sample was cleaned by repeatedly exposing it to 1 atm of hydrogen at 500°C and evacuating the surface reaction products prior to each set of experiments [9].

Optical microscopy of the sample after the completion of experiments showed it to be comprised of coarse grains, about 20% of which had average diameters of 1 mm or larger. An average ASTM grain size of 5 was estimated for the specimen. Laue x-ray diffraction patterns taken on various spots on the sample indicated no preferred orientation. In one instance, a well defined pattern characteristic of a high index plane (a (429) orientation) was observed. This was probably due to diffraction from one or more of the larger grains.

Because of the allotropic transition of iron at 914°C and the presence of trace impurities in the bulk, the preparation of an atomically clean and well annealed surface is a difficult and time consuming task [10]. The most efficient process was found to consist of repeated cycles of argon ion sputtering and annealing in vacuum at 500-600°C. A typical Auger spectrum of the cleaned and annealed surface is shown in Fig. 2. During the permeation runs, the coverage of surface contaminants, as determined by AES, did not increase appreciably for temperatures as low as 100°C.

In order to improve the signal to noise ratio and the mass peak resolution, deuterium was generally substituted for hydrogen in these experiments. No isotope effects on activation enthalpies were detected outside the limits of experimental error, in agreement with the work of Quick and Johnson [11].

2.2 Experimental Measurements

Total pressure measurements by an ionization gauge as well as partial pressure measurements by the QMS when it was directly installed in the main chamber proved inadequate for permeation experiments. These

measurements were affected by spurious effects due to permeation through the steel walls of the cell and back-streaming of previously pumped gases from the ion pump. Similarly, measurements by the differentially pumped QMS were affected by the pressure build up in the main chamber, despite the apparent constancy of the detector chamber ion gauge reading. Typical QMS outputs for two different sample positions are shown in Figure 3. Curves a and b correspond to deuterium fluxes through the QMS analyzer with the sample facing the detector chamber orifice and at an angle of 120° from that position, respectively. The difference curve, designated as c, is taken to represent the flux through the iron sample.

The isothermal variation of the permeation flux with inlet-side hydrogen pressure followed Sievert's law [8], between 380-1250 torr.

An Arrhenius plot of the steady state deuterium flux vs. temperature is presented in Figure 4 for two different runs. A linear regression analysis of the experimental data down to 225°C yields an activation energy for permeation equal to 8.5 ± 0.4 kcal/mole (95% confidence), which is in close agreement to the values reported by Miller et al. [8], Quick and Johnson [11], and Nelson and Stein [9] (8.10, 8.52-8.78, and 8.21 kcal/mole, respectively), in high purity iron samples. No attempt was made to calibrate the mass spectrometer sensitivity for deuterium. The data are presented as normalized relative to the 1/T=0 intercept of the Arrhenius plot evaluated from the above linear regression analysis. The agreement among the above values of the activation energies, despite differences in the surface conditions, indicates that at high temperatures the activation energies for permeation and diffusion are not influenced by surface processes. Assuming the heat of solution of deuterium in iron to be 6.5 kcal/mole [14], we calculate the activation energy for diffusion (see below), to be 2.0±0.4 Kcal/mole.

At temperatures below 200°C, the measured permeation curve falls below the value extrapolated from the high temperature data. The cleanliness of the surface, as monitored by AES, precludes the effect of surface contaminants as a possible explanation of this observation. In the following section, we develope an explanation for this behavior based on the desorption rate of hydrogen from the exit surface of the membrane as a rate controlling factor.

3. Discussion

3.1 Kinetic Model

In the usual treatment of the problem of hydrogen transport through solids, it is implicitly assumed that the only kinetic process controlling the rate of permeation is bulk diffusion through the permeation membrane. In other words, it is assumed that diffusing atoms recombine and desorb as molecules in a comparatively short time upon arriving at the exit interface. An examination of the kinetics of hydrogen desorption from a number of low-index, clean iron surfaces[10,13], indicates that contrary to the above assumption, desorption may indeed become the rate determining step in the permeation process at low temperatures.

A relation accounting for the dependence of the permeation rate on desorption kinetics will be developed based on the potential energy diagram shown in figure 5. Here, the potential energy of a hydrogen atom is shown as a function of distance across the permeation wall. The zero of energy is taken as a hydrogen molecule in the gas phase. The potential wells at each surface represent the sites for stable chemisorption as

hydrogen atoms. The series of minima between these chemisorption wells represent stable sites in the bulk. The intervening maxima represent the barriers surmounted in bulk diffusion.

Under steady state conditions, Fick's first law for one-dimensional transport through the bulk of a solid is normally stated as [18]:

$$J = D(C_1 - C_2/L) \tag{1}$$

Where J = Steady state flux ($cm^{-2}.sec^{-1}$),

D = Diffusion coefficient ($cm^2.sec^{-1}$),

C_1, C_2 = Volume concentrations of the diffusing species at the planes just below the entrance and exit interfaces of the permeation wall, respectively (cm^{-3}),

L = wall thickness (cm).

We will assume that the concentration in the near-surface side of the membrane is in equilibrium with the gas phase and write, using Sievert's law:

$$C_1 = SP^{\frac{1}{2}} \tag{2}$$

where the solubility, S ($cm^{-3}.atm^{-\frac{1}{2}}$), is a function of temperature.

The gas-phase pressure on the outlet side was always maintained at or below 10^{-7} torr. In the absence of surface effects this leads to $C_2 \sim 0$ and:

$$J = DSP^{\frac{1}{2}}/L \tag{3}$$

(we shall see that surface effects can raise C_2 to a finite value, approaching C_1 at low enough temperatures).

We will also make a change in notation, for convenience in the kinetic analysis in that we will state the hydrogen concentrations in terms of n_i, atoms per cm^2, on any plane parallel to the interface. That is,

$$C_i = \tfrac{1}{2}(n_i/d) \tag{4}$$

where d is the interplanar spacing. The factor of $\frac{1}{2}$ is necessary to account for the fact that permeation data are usually expressed on a per H_2 molecule basis.

Mass balance expressions for the Hydrogen atom fluxes onto and away from planes 2 and 3 (as defined in Figure 5), at steady state (i.e. $dn_2/dt=dn_3/dt=0$), may be written as:

$$D(n_1-n_2)/2Ld + \tfrac{1}{2}k_{32}n_3 - \tfrac{1}{2}k_{23}n_2(1-n_3/n_o)=0 \tag{5}$$

$$\tfrac{1}{2}k_{23}n_2(1-n_3/n_o) - \tfrac{1}{2}k_{32}n_3 - k_d(n_3)^2=0 \tag{6}$$

where:

$n_1 = 2SP^{\frac{1}{2}}$

n_o = number of surface sites per unit area available to hydrogen adsorption (cm^{-2}),

k_{ij} = probability for transition of a hydrogen atom from a site on plane i to a site on plane j (sec^{-1}),

k_d = desorption probabilty (cm^2sec^{-1}).

The parameter $(1-n_3/n_o)$ in the above equations expresses the assumption that a site on plane 3 already occupied by an adsorbed hydrogen atom is unavailable to other hydrogen atoms attempting to arrive on that plane. A similar term for plane 2 can be neglected if we assume $n_2 << n_o$.

Simultaneous solution of equations 5 and 6 yields:

$$A_1(n_3)^3+A_2(n_3)^2+A_3n_3+A_4 = 0 \qquad (7)$$

where $$A_1 = k_d/n_o, \qquad (7a)$$

$$A_2 = -k_d[1-(D/Ldk_{23})], \qquad (7b)$$

$$A_3 = -(SP^{\frac{1}{2}}D/n_oL)-(\tfrac{1}{2}k_{32}D/Ldk_{23}) \qquad (7c)$$

$$A_4 = SP^{\frac{1}{2}}D/L \qquad (7d)$$

The steady state permeation flux, J, can be expressed in terms of n_3 as:

$$J = k_d(n_3)^2, \qquad (8)$$

with n_3 obtained from the solution of Equation 7.

These equations contain five temperature-dependent terms, namely:

$$S = S_o \exp(-\Delta H_{sol}/RT)$$

$$D = D_o \exp(-\Delta H_{dif}/RT)$$

$$k_{23} = k_{23}^o \exp(-\Delta H_{23}/RT)$$

$$k_{32} = k_{32}^o \exp(-\Delta H_{dis}/RT)$$

$$k_d = K_d^o \exp(-\Delta H_{des}/RT)$$

where the relevant activation energies are shown in Figure 5.

For the case of hydrogen in iron, $\Delta H_{23} \sim \frac{1}{4}\Delta H_{dif} \sim 1$ Kcal/mole (the activation energy for diffusion, ΔH_{dif}, is usually expressed on a per molecule basis; we have assumed the transition from the subsurface site to the adsorbed state to be equivalent to a diffusive jump and have therefore, included the factor of $\frac{1}{4}$ to account for the change to a per atom basis), and $k_{23}^o = D_o/a_o^2$, where D_o and a_o are the pre-exponential for the diffusion coefficient and the bcc lattice constant, respectively (see Section 3.2). Thus, the second term in the expression for A_2 (Equation 7b) may be expressed as:

$$D/LdK_{23} = (a_o^2/Ld)\exp(-\Delta H_{dif}/2RT)$$

which, at all temperatures, is negligibly small when compared to unity. Hence:

$$A_1(n_3)^3/A_2(n_3)^2 \sim -n_3/n_o$$

Moreover, our calculations show that $-A_3n_3/A_4$ becomes a negligibly small number at high temperatures (see Section 3.2). Therefore, at these temperatures, where n_3/n_o is also found to be small, Equation 7 reduces to:

$$-k_d(n_3)^2 + SP^{\frac{1}{2}}D/L = 0$$

leading to:

$$J = SP^{\frac{1}{2}}D/L$$

the classical relation for this case.

3.2 Application to Hydrogen in Iron

In applying the above treatment to the case of hydrogen in iron, the crystallographic parameters d and n_o are calculated as usual. The value of C_1 at one atmosphere was calculated according to the solubility expression recommended by Gonzales [14].

$$C_1 = SP^{\frac{1}{2}} = 9X10^{19} \exp(-6.5/RT) \qquad (9)$$

where R is expressed in Kcal/mole.

Previous studies of the desorption of hydrogen from iron, made on clean (110), (100) and (111) surfaces [10,13] have yielded the desorption energies summarized in Table 1. There is a significant variation both with the crystal face and with adlayer coverage. These values do, however, establish an envelope of possible behavior on these faces. The question of

what value to use for faces of arbitrary origin remains. However, studies in a wide range of systems [22] have indicated that the presence of defects such as steps or kinks generally increase the activation energy for desorption by 1-4 Kcal/mole. In the absence of specific data for vicinal iron surfaces, we will assume that these iron surfaces will follow the same pattern and will exhibit higher desorption activation energies than the corresponding flat surfaces. On the basis of this arguement, and keeping in mind that the magnitude of ΔH_{des} is coverage-dependent on the terrace sites [10,22], we have assumed for the present calculations, that 26 Kcal/mole (see Table 1) is the upper limit for the desorption energy on vicinal surfaces over the full range of coverage. Values of ΔH_{des} for low index surfaces were chosen according to Table 1. The frequency factor for desorption was taken as 2×10^{-3} cm^2/sec [13], leading to:

$$k_d = 2.0 \times 10^{-3} \exp (- \Delta H_{des}/RT). \qquad (10)$$

The transition of a hydrogen atom from a subsurface site on plane 2 to an adsorption site on plane 3 was assumed to be equivalent to a transition from one interstitial site to another - i.e. a diffusive jump. Therfore, ΔH_{23}, the activation energy per hydrogen atom, was taken as half of the activation energy for diffusion, ΔH_{dif}. Similarly, the frequency factor for this process was evaluated using the expression for D_o in a bcc lattice [15], yielding:

$$k_{23} = D_o(a_o)^{-2} \exp (- \Delta H_{dif}/2RT) \qquad (11)$$

The activation energy for transition from a site on plane 3 to a site on plane 2 is estimated as:

$$\Delta H_{dis} = \tfrac{1}{2}(\Delta H_{sol} + \Delta H_{dif} + \Delta H_{des}) \qquad (12)$$

per atom of hydrogen, with the implicit assumption that the activation energy for chemisorption is small enough to be neglected [13]. The frequency factor for this process is calculated simply by multiplying the frequency factor for the second order desorption process by n_o, yielding:

$$k_{32} = 3.4 \times 10^{12} \exp (- \Delta H_{dis}/RT) \qquad (13)$$

Equation 7 may now be solved numerically if an expression for either the diffusion coefficient or the permeation rate is available. We used the activation energy obtained in the present study and examined various values for the activation energy for desorption in order to obtain a best fit to our data. The solution of Equations 7 and 8 for ΔH_{des} = 25 Kcal/mole, up to a saturation coverage of 1 monolayer, was found to agree well with the experimental results, as shown by the solid curve in Figure 4. Due to the polycrystalline nature of the sample, the origin of this value for ΔH_{des} is not clear. However, it is in good agreement with the upper limit of the energies postulated above for vicinal orientations.

We also performed calculations in order to make a comparison between the predictions of the present model and the previously obtained experimental data for the apparent diffusivity of hydrogen in iron. The scatter in the values as reported in the literature is quite large even at

temperatures above 200°C [1]. However, in comparing the diffusivity data obtained under different surface conditions, we have already shown that such differences should not appreciably affect the permeation rate of hydrogen at high temperatures. Furthermore, we applied the analysis developed above to the data reported by Nelson and Stein [9] and, using the highest heat of adsorption assumed in the present study, found that the apparent activation energy for permeation at high temperatures increased only by 0.1% over that experimentally measured. Therefore, unless much stronger surface reactions are shown to be operative, the scatter at high temperatures may be attributed to bulk processes or to experimental errors. It is thus sufficient to examine the role of the clean surface effects on representative expressions for the permeation rate as obtained from high temperature data.

The range of values for the activation energy and the pre-exponential factor obtained for the permeation of hydrogen in high purity and well annealed iron samples, as well as the solubility parameters corresponding to each experiment, are shown in Table 2. Due to the range of values for ΔH_{des} on various surfaces, the expected value of the permeation rate at low temperatures will depend on the surface structure of the sample. Thus, Equations 7 and 8 may be solved for the range of the desorption energies and the coefficient of permeation at high temperatures, to develope an envelope for the expected values of the hydrogen flux through the sample as a function of temperature. The resulting plot is shown in Figure 6, where we have plotted $(JL/P^{\frac{1}{2}})$ vs 1/T. The broken lines correspond to the predicted values of the permeation flux for various desorption energies while the different solid lines correspond to the different permeation parameters as listed in Table 1.

Values of the apparent diffusivity can now be evaluated based on Equation 3, which was derived solely on the basis of solubility - bulk transport considerations. The range of apparent diffusivities predicted for different permeation-desorption enthalpy combinations is shown as the cross hatched area in Figure 7. The range of experimental data reported in Reference 1 is also shown in this figure as the dotted region.

The experimental data in Figure 7 also include values obtained under transient conditions, during permeation experiments. Kiuchi and McLellan [6] have carried out a statistical study of the pertinent data in the literature. They conclude that permeation transient analyses are more seriously affected by surface conditions. This may be expected, as in the analysis of permeation transients the concentration at plane 2 (Figure 5) is usually assumed to be independent of both time and temperature [18,20]. This assumption, according to the results of the present study, is clearly invalid. Provided that the sample geometry allows for a one dimensional analysis of permeation, this analysis should be performed in accordance with the considerations leading to equations 5 and 6. In the absence of such considerations, the transient experiments may lead to the prediction of values of apparent diffusivity lower than those obtained under steady state but otherwise similar experimental conditions[6].

Interesting features are distinguishable in Figure 6. The deviation from Arrhenius behavior occurs quite abruptly. Therefore, the value of the true activation energy for permeation may be reliably found by linear regression analysis of the high temperature data. At temperatures just below the point of deviation, the hydrogen flux is controlled almost entirely by the desorption kinetics; an evaluation of the activation energy for permeation at low temperatures shows it to be equivalent to

that for hydrogen desorption. Hence, if Equation 3 is applied to the low temperature permeation data anomalously high values of the apparent activation energy for diffusion - equivalent to $\Delta H_{des}-\Delta H_{sol}$ - will be obtained (Figure 7). This deviation from Arrhenius behavior is clearly shown to occur at higher temperatures for planes which adsorb the hydrogen atom more strongly. On the other hand, the outcome of the present analysis was not sensitive to the numerical choice of ΔH_{dis} (Equations 7 and 12). Changing the assumed value of this parameter by as much as ±20%, did not appreciably affect the results.

Figure 8 shows the effect of the permeation wall thickness on the value of the apparent diffusivity, as predicted by the present analysis. The corresponding variations of the permeation rate are also shown as vertical bars in Figure 7. The calculated value of diffusivity approaches its value expected from extrapolation of the high temperature measurements as the wall thickness increases, causing the bulk transport process to become dominant in the determination of the overall rate of permeation.

The combined effects of the sample thickness and the heat of desorption on the temperature at which deviation from Arrhenius behavior is observed may be expressed in terms of a deviation temperature, T_D which may be estimated by equating the Einstein time for diffusion, τ_E and the mean stay time for adsorption, τ_d, yielding:

$$T_D=[(\Delta H_{des}-\Delta H_{dif})/R][\ln(L^2 k_d{}^o n_o/2D_o)]^{-1}$$

In most studies, however, an independent determination of the desorption parameters included in the above expression is not possible, and T_D has to be determined empirically.

The trend is similar to that reported by Wach and Miodownik [17] in their electrochemical permeation study at 25°C. Similarly, Palczewska and Ratajczk [12] considered the effect of wall thickness on gas permeation between 30-40°C. They report that diffusivity is independent of membrane thickness above 0.78 mm, while for thicknesses below 0.42 mm, decreased values of apparent diffusivity are observed. Nelson and Stein [9] also studied the influence of wall thickness on permeation for temperatures of 240°C and higher. By geometrical arguments they concluded that, based on that part of their study, permeation was not influenced by surface processes. However, since the data used in their analysis describe the permeation behavior above the deviation temperature observed in their experiments (100°C), they are outside the range in which the permeation rate is affected by surface processes and thus do not provide a critical test of the effect of these surface processes on permeation.

Surface contaminants may also lead to the observation of incorrect values of the apparent diffusivity if their presence results in the retardation or enhancement of the desorption process. For example, pre-adsorbed submonolayers of sulfur, oxygen and carbon were observed to decrease both the energy and the frequency factor for desorption of hydrogen from Fe(100) surfaces while pre-adsorbed potassium seemed to increase the value of the former [21]. Direct evidence for this effect was observed for the permeation of hydrogen in palladium in an electrochemical permeation study [23]. In that investigation it was noticed that sulfur deposition on the membrane surface resulted in reduced permeation flux and consequently low values for the apparent diffusivity.

3.3 Results for Other Metals

Among the transition metals, the interaction of iron, nickel and palladium with hydrogen has received considerably more attention than others. Therefore, a comparison of the results for iron may be most appropriate with those for the latter two metals. The diffusivity values obtained by various permeation methods for these metals do not indicate the anomalies observed for iron, even at room temperature or below [1].

Hydrogen permeation in nickel was examined using the model developed in the present study. Because of the consistency in the values of diffusivity reported by various authors [1], it is sufficient to consider the experimental results of only one study. For this purpose we selected the work of Ebisuzaki et al [24a] for the permeation parameters. Those parameters relevant to the desorption of hydrogen from various nickel surfaces were taken from the work by Christmann et al. [24b] (see Table 3). The analysis showed excellent agreement with the experimental data of Ebisuzaki et al. [24a]. A deviation from Arrhenius behaviour was predicted only for temperatures lower than -20°C, for the highest reported heat of desorption as applied to vicinal surfaces (see above).

Similar to nickel, there is good consistency among various experimental values of hydrogen diffusivity in palladium [1]. There is, however, substantial evidence that hydrogen adsorption on this metal is more complex than that shown by the potential energy diagram of Figure 5. Adsorbed Hydrogen atoms are observed to readily occupy subsurface sites on Pd(111) surfaces [25a,b] while desorption from Pd(100) surfaces was observed to follow "quasi first order" kinetics beyond very low coverages [25c], in contrast with iron [10,13]. Therefore, the present model can not give an adequate description of the effect of the desorption kinetics on hydrogen permeation in palladium. In spite of the above evidence, Engel

and Kuipers [25d] found that a potential energy diagram similar to that used in this study - with parameters chosen to yield a best fit to the experimental data - adequately described their results on the interaction between hydrogen and deuterium on a Pd(111) surface for temperatures above 75°C. Their study indicated that transport between the surface and the bulk is an important factor for hydrogen adsorption on the Pd(111) surface.

We have also attempted to apply the kinetic model developed here to the case of hydrogen in palladium, by curve fitting, using the values of k_{32}^{o} and k_{d}^{o} as the fitting parameters. The values of all other parameters involved in Equation 7 were taken from the literature [25e,25f]. The value of k_{d}^{o}, which gave a reasonable fit to the experimental measurements of Koffler et al. [25e] on hydrogen permeation in palladium, was approximately one order of magnitude larger than the values of k_{d}^{o} for either iron or nickel; while k_{32}^{o} was found to be smaller than the values for nickel and iron by the same ratio (see Table 3). The equation developed in this fitting process predicts an anomalous decrease in the value of diffusivity, similar to that found in iron, for temperatures below 75°C for vicinal surfaces, i.e. for ΔH_{des} independent of surface coverage (see the previous section). We have found no experimental studies which report such a deviation. Only contaminated surfaces showed a value of the apparent diffusivity below that expected from the extrapolation of the high temperature data, as mentioned above [23]. The reason for this lack of agreement is not obvious, but may be related to the existence of a strongly-bound subsurface hydrogen site.

Perhaps the most straightforward experimental extension of the present work would be to measure the work function variation of the exit surface as a function of time and temperature, in ultrahigh vacuum, during a permeation experiment. Hydrogen adsorption is known to change the electron work function of various surfaces of iron and other metals in a manner determined by the surface structure [10,22b]. This occurs due to surface dipoles formed in the electronic interaction between the adsorbate and the adsorbent species. Therefore, if the desorption kinetics do become the dominant step in the overall rate of hydrogen permeation at low temperatures, the variation in the adlayer coverage as a function of time or temperature should directly result in changes in the work function of the sample. Of course, in such experiments it would be necessary to account for temperature effects on the work function.

4. Conclusions

1. Steady state permeation measurements of deuterium in a high purity, polycrystalline iron sample, having an atomically clean exit surface, have shown a deviation from Arrhenius behavior at temperatures below 200°C.

2. This deviation can be accounted for by a model in which the known desorption kinetics of hydrogen from iron are included as an additional impediment to the permeation flux.

3. The model developed also provides a good explanation of low apparent diffusivities observed in previous studies of hydrogen permeation through iron.

4. The model is also in good agreement with previous studies of hydrogen permeation through nickel, but does not fit previous results for palladium.

Acknowledgement

This work was supported in part by ARO under Contract Number DAAL03-86-K-0076, and in part by the chemistry program of ONR. This support is gratefully acknowledged.

TABLE 1 [10]

Plane	Coverage (atoms/site)	Desorption Energy (Kcal/mole)
(100)	$0 < \Theta < 0.5$	26
	$0.5 < \Theta < 1$	<26
(100)	$0 < \Theta < 0.2$	24
	$0.2 < \Theta < 1$	18
(111)	$0 < \Theta < 0.45$	21
	$0.45 < \Theta < 0.85$	18
	$0.85 < \Theta < 1.0$	13

TABLE 2

Parameters for hydrogen permeation in high purity iron

	Permeability (H_2/cm.sec.atm$^{\frac{1}{2}}$)	Solubility (H_2/cm^3.atm$^{\frac{1}{2}}$)	Ref.
I-	$6.2 \times 10^{17} \exp(-4130/T)$	$2.7 \times 10^{20} \exp(-3323/T)$	[9]
II-	$1.3 \times 10^{17} \exp(-4288/T)$	$1.6 \times 10^{20} \exp(-3442/T)$	[11]
III-	$9.2 \times 10^{16} \exp(-4074/T)$	$9.0 \times 10^{19} \exp(-3270/T)$	[8]

Table 3

Parameters for Hydrogen Permeation in Nickel and Palladium

	ΔH_{sol}	ΔH_{dif}	ΔH_{des}	k_d^o	k_{32}^o
	——Kcal/mole——			cm^2/sec	sec^{-1}
Ni	3.6(a)	9.6(a)	23(b)	$8x10^{-2}$(c)	$n_o k_d$(f)
Pd	-2.0(d)	5.7(d)	23(c)	$8x10^{-1}$(e)	$7x10^{12}$(e)

a- Ref. 24a

b- Ref. 24b

c- Ref. 25f

d- Ref. 25e

e- adjusted parameters (see text)

f- see Section 3.2

References

1- J. Völkl and G. Alefeld in Hydrogen in Metals I, ed. J. Völkl and G. Alefeld, Springer - Verlag, Berlin (1978) chapter 12,

2- R. A. Oriani, Acta Metall., 18 (1970) 147,

3- S. Hiotani and Y. Ohmori, Trans. Japan Inst. Met., 26 (1985) 622,

4- K. T. Kim, J. K. Park, J. Y. Lee, and S. H. Hwang, J. Mater. Sci., 16 (1981) 2590,

5- K. Ono and L. A. Rosales, Trans. Metall. Soc. AIME, 242, (1968), 244,

6- K. Kiuchi and R. B. McLellan, Acta metall., 31 (1983) 961,

7- a. D. C. Carmichael, J. R. Hornaday, A. E. Morris, and N. A. Parlee, Trans. Metall. Soc. AIME, 218(1960) 830; b. H. L. Eschbach, F. Gross, and S. Schullen, Vacuum, 13 (1963) 543,

8- R. F. Miller, J. B. Hudson, and G. S. Ansell, Met. Trans. A, 6A, (1975) 117,

9- H. G. Nelson and J. E. Stein, NASA Technical Note TN D-7265 (1973),

10- F. Bozso, G. Ertl, M. Grunze, and M. Weiss, Appl. Surf. Sci., 1 (1977) 103,

11- N. R. Quick and H. H. Johnson, Acta Metall., 26 (1978) 903,

12- W. Palczewska and I. Ratajczyk, Bull. Acad. Pol. Sci. Ser. Chim., 9 (1961) 267,

13- E. A. Kurz, PhD Thesis, Rensselaer Polytechnic Inst. (1986),

14- O. D. Gonzalez, as quoted in ref. 8,

15- J. W. Christian, The Theory of Transformation in Metals and Alloys: An Advanced Textbook in Physical Metallurgy, 2nd edition, Pergamon Press, Oxford (1975),

16- A. J. Kumnick and H. H. Johnson, Acta Metall., 28 (1980) 33,

17- S. Wach and A. P. Miodownic, Corr. Sci., 8 (1968) 271,

18- J. Crank, The Mathematics of Diffusion, 2nd edition, Clarendon Press, Oxford (1975) chapter 4,

19- H. G. Ellerbrock, G. Vibrans, and H. P. Stüwe, Acta Metall. 20 (1972) 53,

20- H. G. Lotz, G. Schulzek, and H. Viefhaus, Appl. Surf. Sci., 5 (1980) 216,

21- J. Benziger and R. J. Madix, Surf. Sci., 94 (1980) 119,

22- a. G. Ertl, in The Nature of The Surface Chemical Bond, T. N. Rhodin and G. Ertl ed. North- Holland (1979) chapter 5; b. B. Poelsema, G. Mechtersheimer, and G. Comsa, Surf. Sci., 111 (1981) 519; c. B. J. J. Koelman, S. T. deZwart, A. L. Boers, B. Poelsema, and L. K. Verhey, Nucl. Inst. Meth. Phys. Res., 218 (1983) 225; d. H. Nozoye, Surf. Sci., 169 (1986) L362,

23- R. V. Bucur, Int. J. Hydrogen Energy, 10 (1985) 399,

24- a. Y. Ebisuzaki, W. J. Kass, and M. O'Keeffe, J. Chem. Phys., 46 (1967) 1378; b. K. Christmann, O. Schober, G. Ertl, and M. Neuman, J. Chem. Phys., 60 (1974) 4528,

25- a. T. E. Felter, S. M. Foiles, M. S. Daw, and R. H. Stulen, Surf. Sci., 171 (1986) L379; b. G. D. Kubiak and R. H. Stulen, J. Vac. Sci. Technol. A, 4 (1986) 1427; c. R. G. Behm, K. Christmann, and G. Ertl, Surf. Sci., 99 (1980) 320; d. T. Engel and H. Kuipers, Surf. Sci., 90 (1979) 162; e. S. A. Koffler, J. B. Hudson, and G. S. Ansell, Trans. Metall. Soc. AIME, 245 (1969) 1735; f. H. Conrad, G. Ertl, and E. E. Latta, Surf. Sci., 41 (1974) 435

Figure Captions

Figure 1a: Ultrahigh vacuum apparatus.

Figure 1b: Permeation cell assembly.

Figure 2: AES spectrum of the cleaned and annealed iron sample.

Figure 3: QMS output for hydrogen permeation at 377°C. a-sample facing the detector chamber orifice, b-sample at 120° from the orifice, c-the difference curve.

Figure 4: Arrhenius plot of hydrogen flux as a function of temperature. The straight line shows the result of the linear regression analysis of data for T>200°C. The solid line indicates the outcome of the analysis based on the model discussed in sec. 3.

Figure 5: Potential energy diagram for hydrogen permeation in iron.

Figure 6: Effect of the desorption energy on hydrogen permeation in iron: a. 26, b. 24, c. 22, d. 20, and e. 18 Kcal/mole. Differences in high temperature values are due to the choice of various permeation parameters (Table 2)

Figure 7: Predicted (cross hatched) and experimental (dotted) [1] values of the apparent diffusivity vs temperature.

Figure 8: Effect of membrane thickness on the ratio of calculated apparent diffusivity, D_{App}, to that extrapolated from the high temperature data, D_{True}.

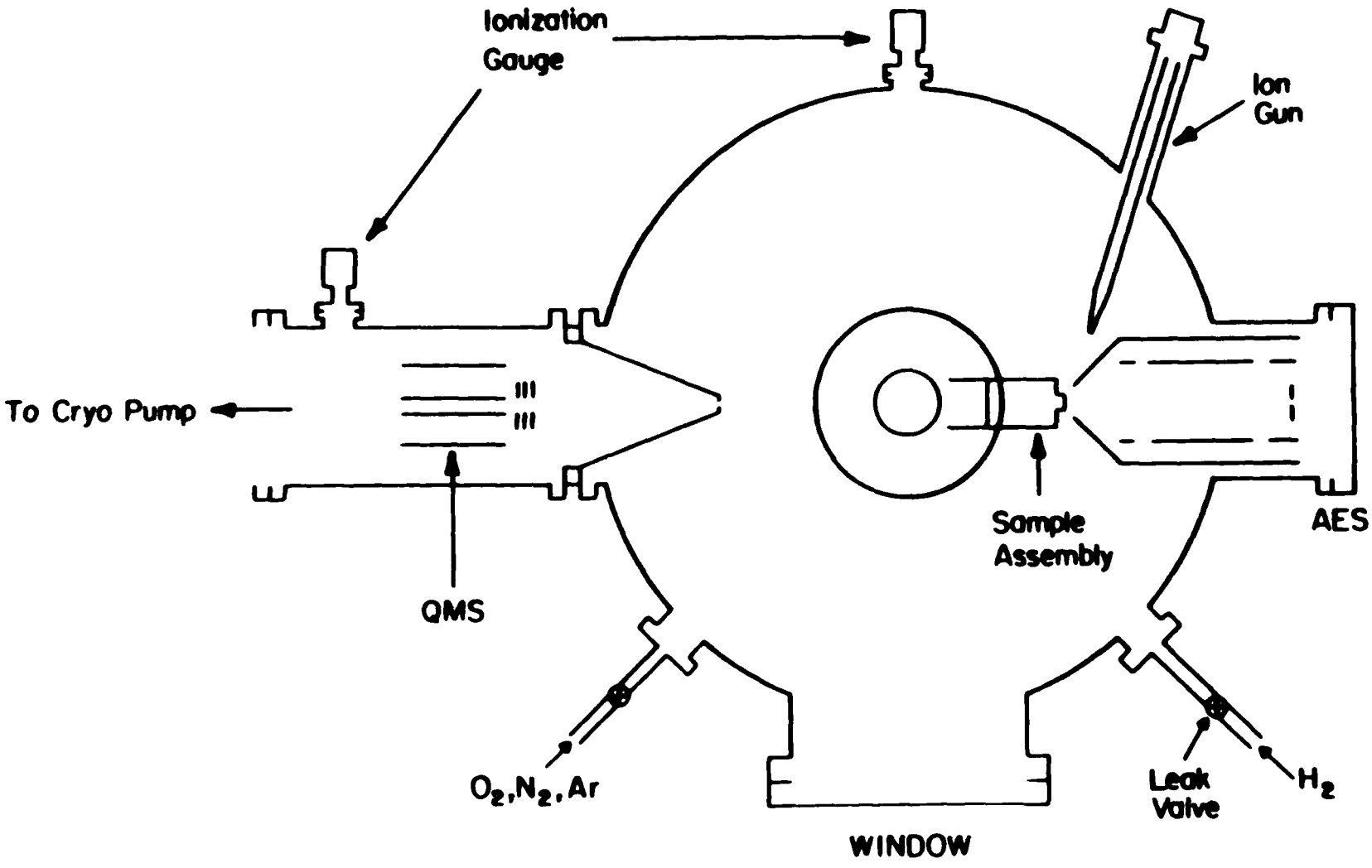
Ionization
Gauge
Ion
Gun
To Cryo Pump
QMS
Sample
Assembly
AES
O_2, N_2, Ar
Leak
Valve
H_2
WINDOW

Fig. 1a

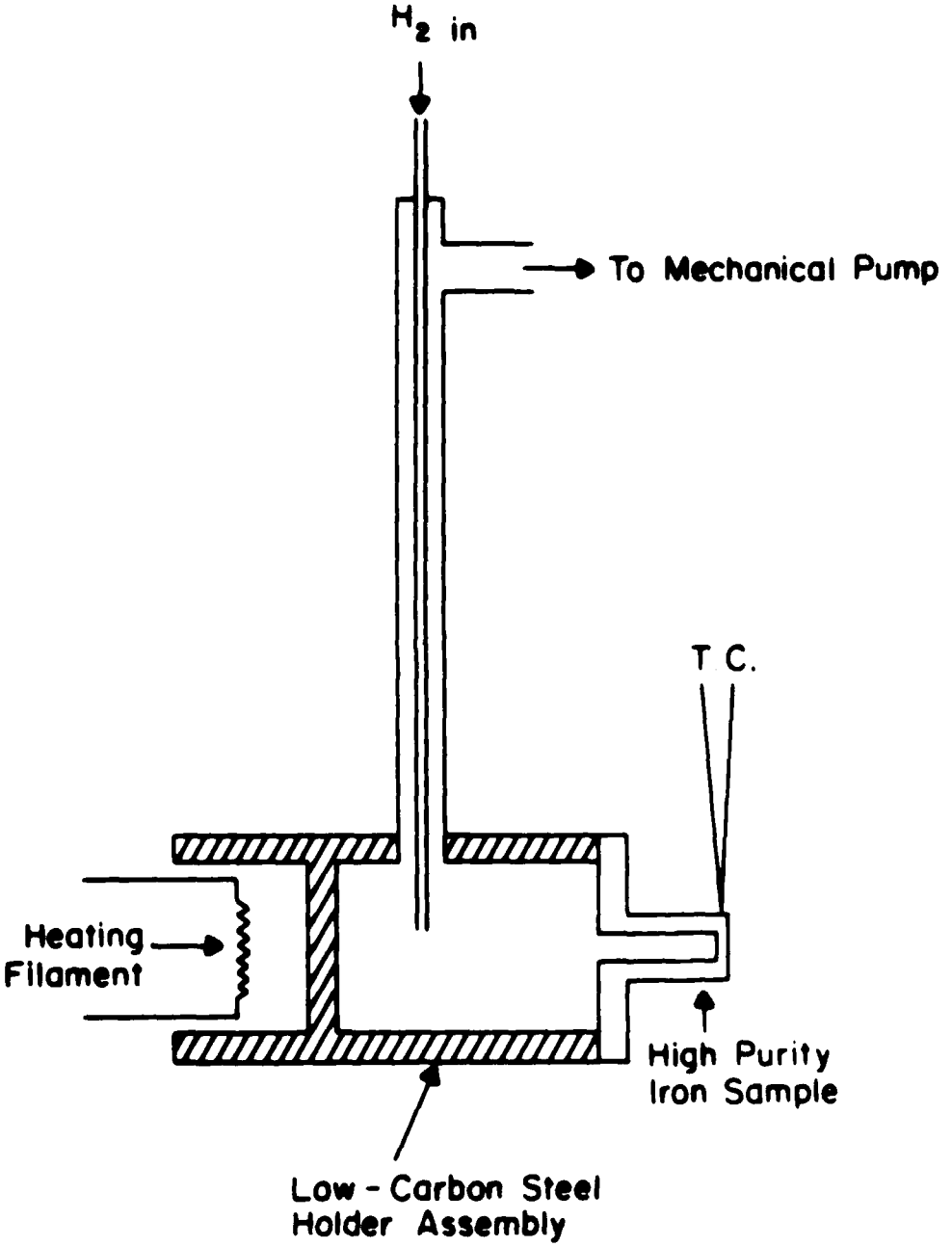
H_2 in
To Mechanical Pump
T C.
Heating Filament
High Purity Iron Sample
Low - Carbon Steel Holder Assembly

Fig. 1b

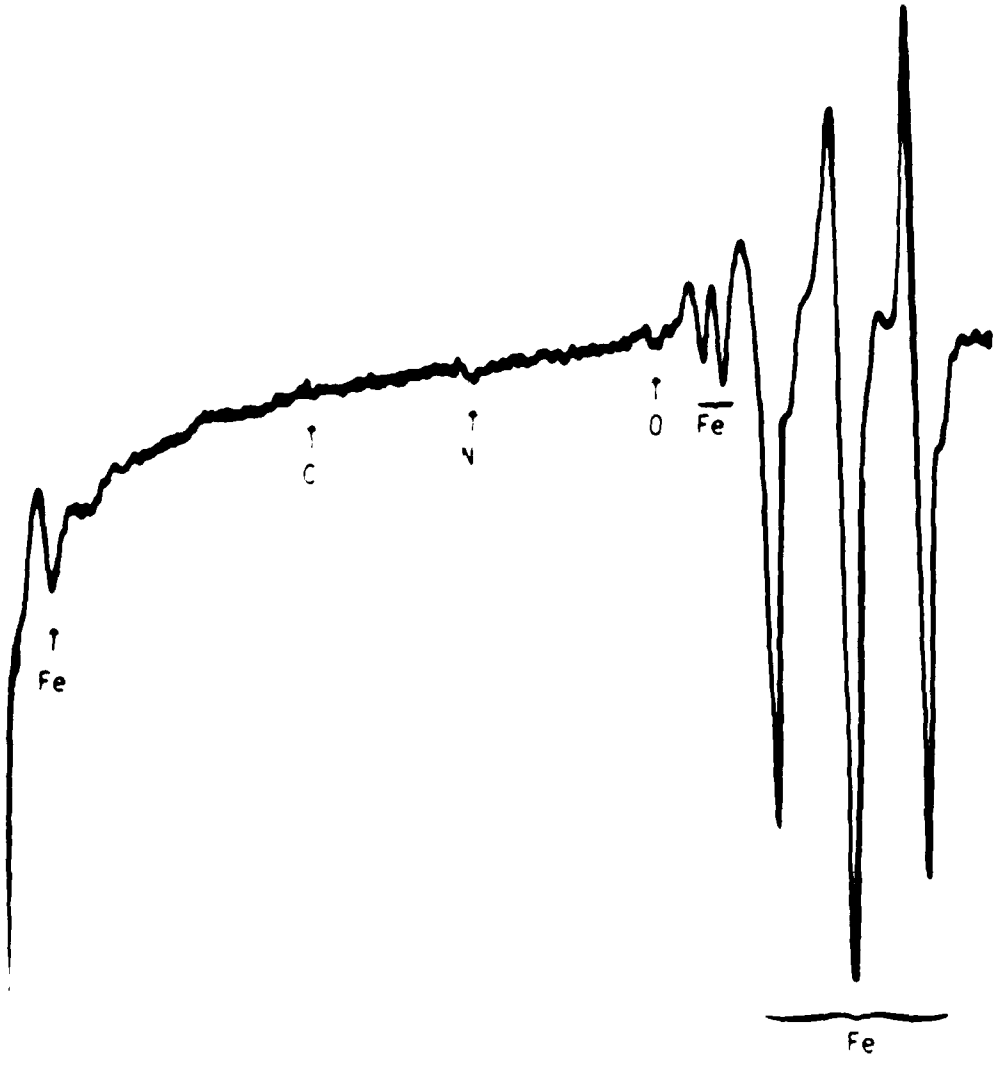
Fe
C
N
O
Fe
Fe

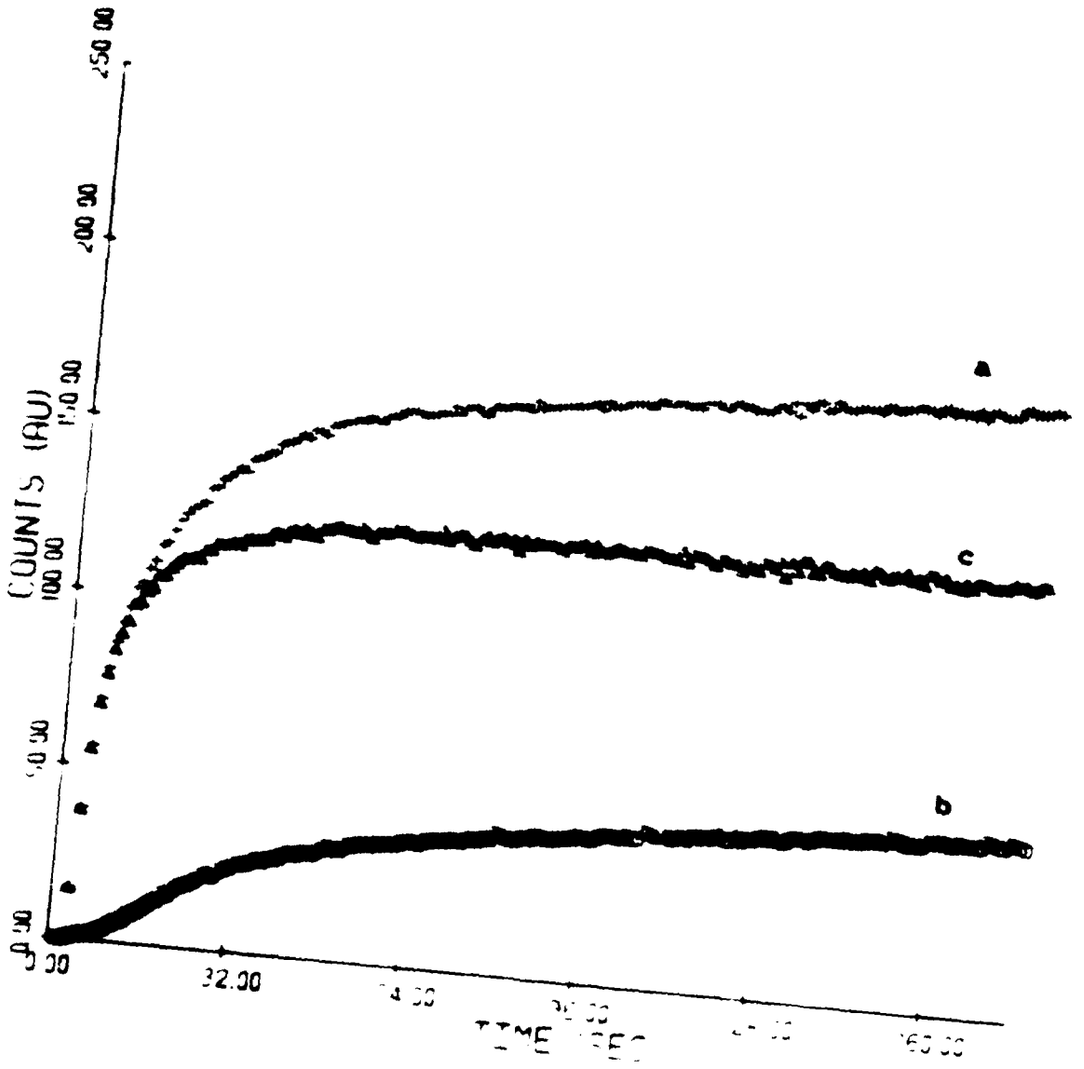

Fig. 3

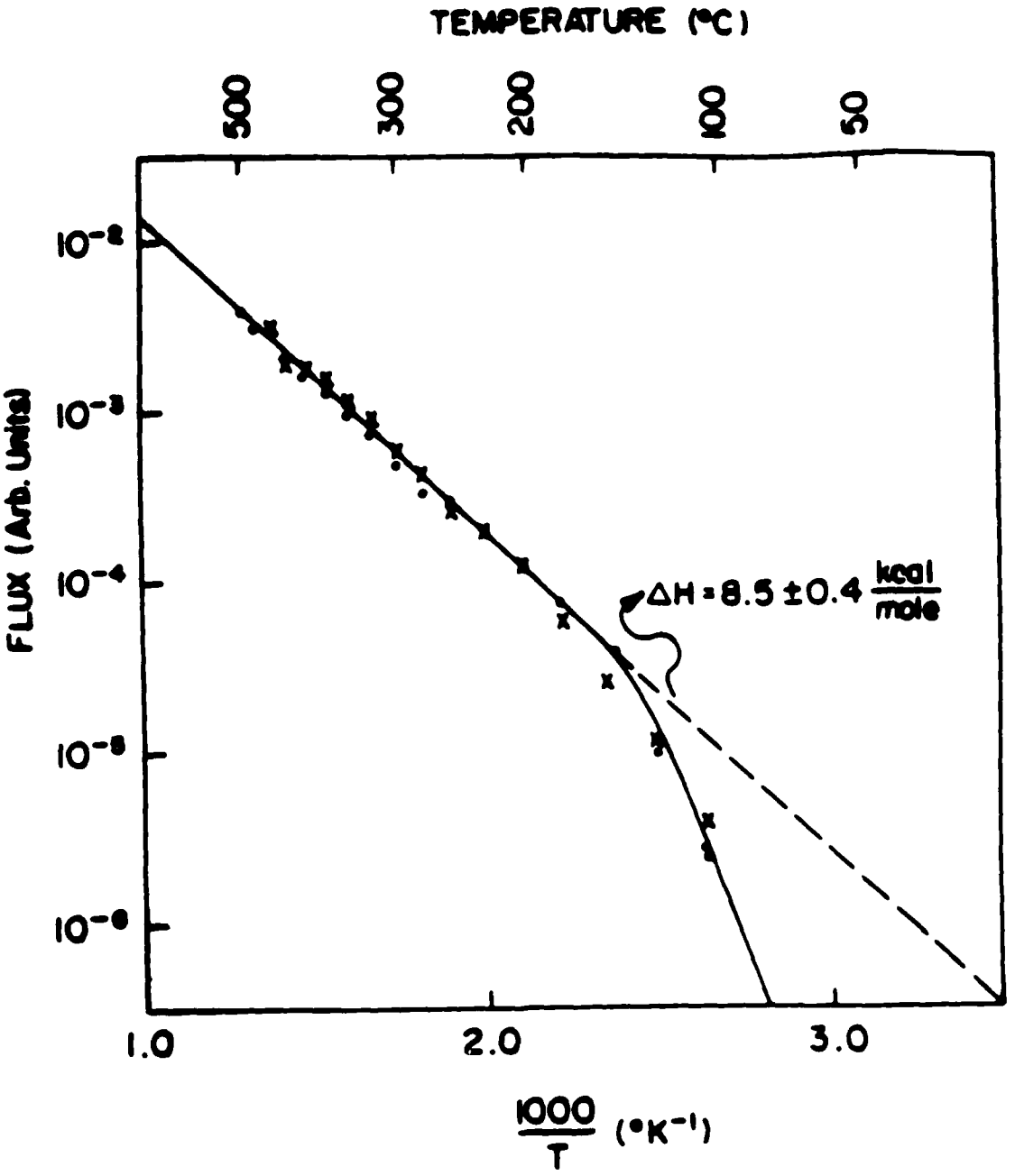
TEMPERATURE (°C)
500
300
200
100
50
FLUX (Arb. Units)
10^{-2}
10^{-3}
10^{-4}
10^{-5}
10^{-6}
ΔH = 8.5 ± 0.4 kcal/mole
1.0
2.0
3.0
1000/T (°K⁻¹)

Fig. 4

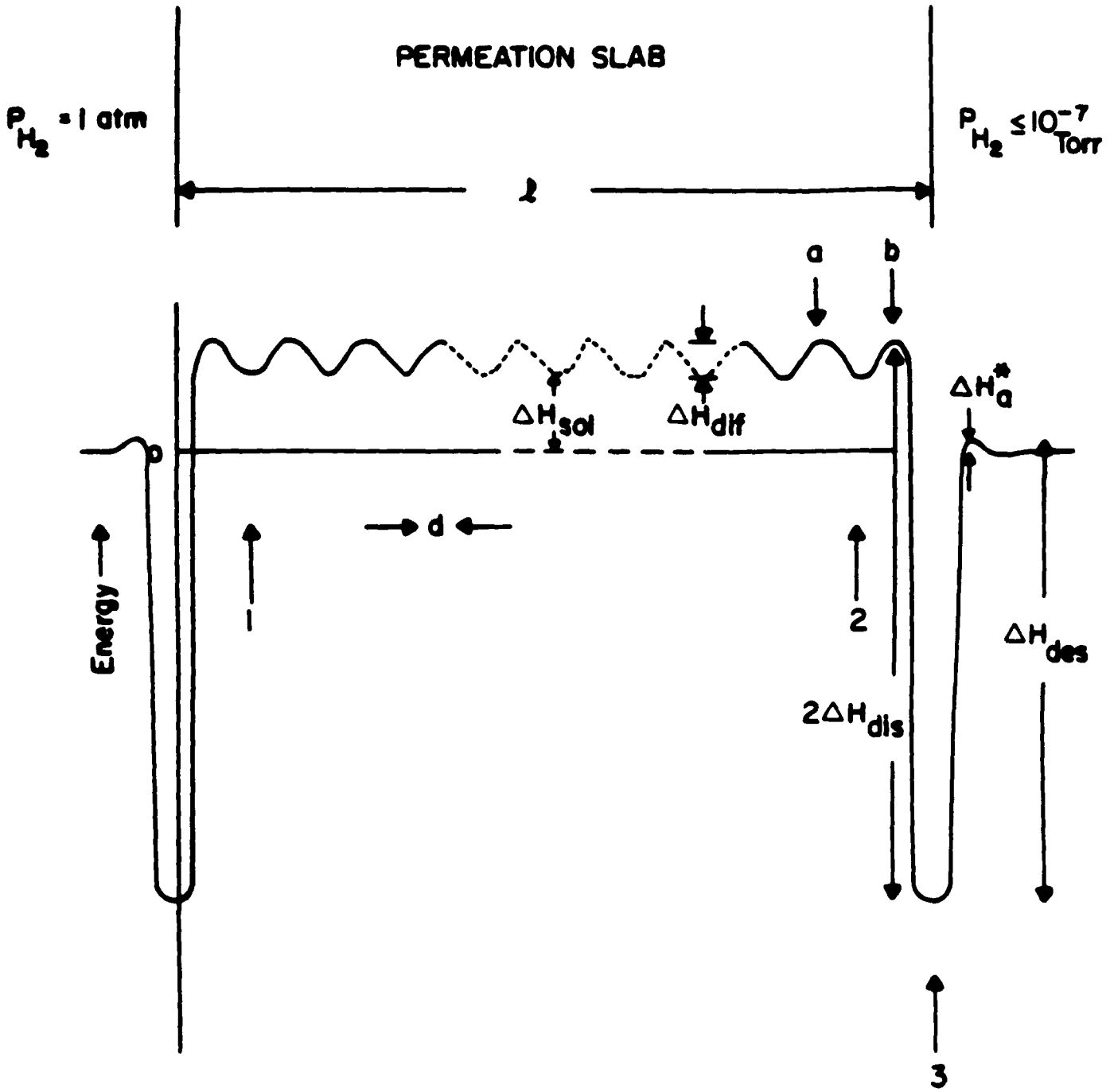
PERMEATION SLAB
P_{H_2} = 1 atm
$P_{H_2} \leq 10^{-7}$ Torr
ℓ
a
b
ΔH_{sol}
ΔH_{dif}
ΔH_a^*
d
Energy
1
2
3
$2\Delta H_{dis}$
ΔH_{des}

Fig. 5

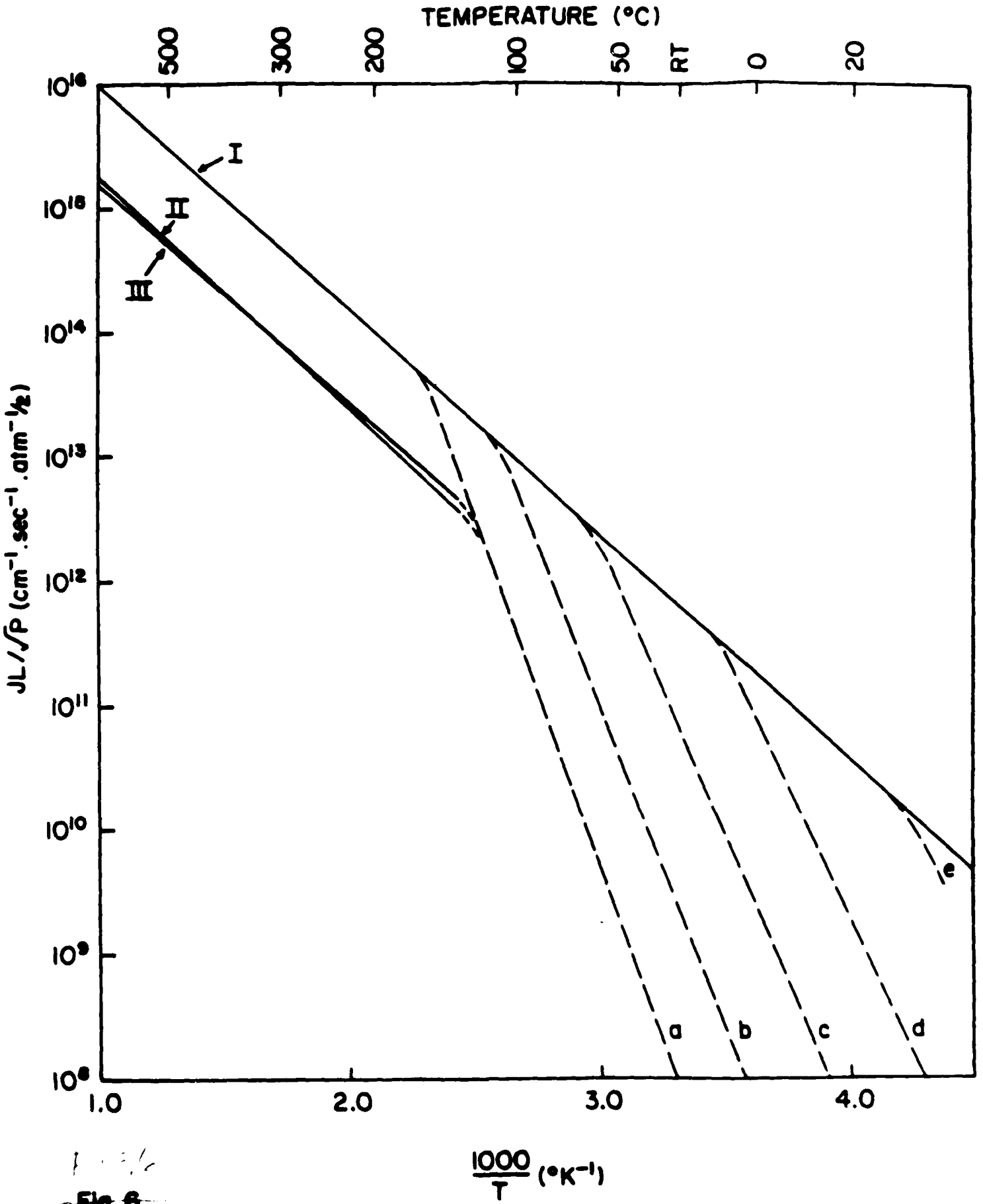
TEMPERATURE (°C)
500
300
200
100
50
RT
0
20
10^{16}
10^{15}
10^{14}
10^{13}
10^{12}
10^{11}
10^{10}
10^{9}
10^{8}
I
II
III
a
b
c
d
e
$JL/\sqrt{P}$ ($cm^{-1}.sec^{-1}.atm^{-1/2}$)
1.0
2.0
3.0
4.0
$\frac{1000}{T}$ ($°K^{-1}$)

Fig. 6

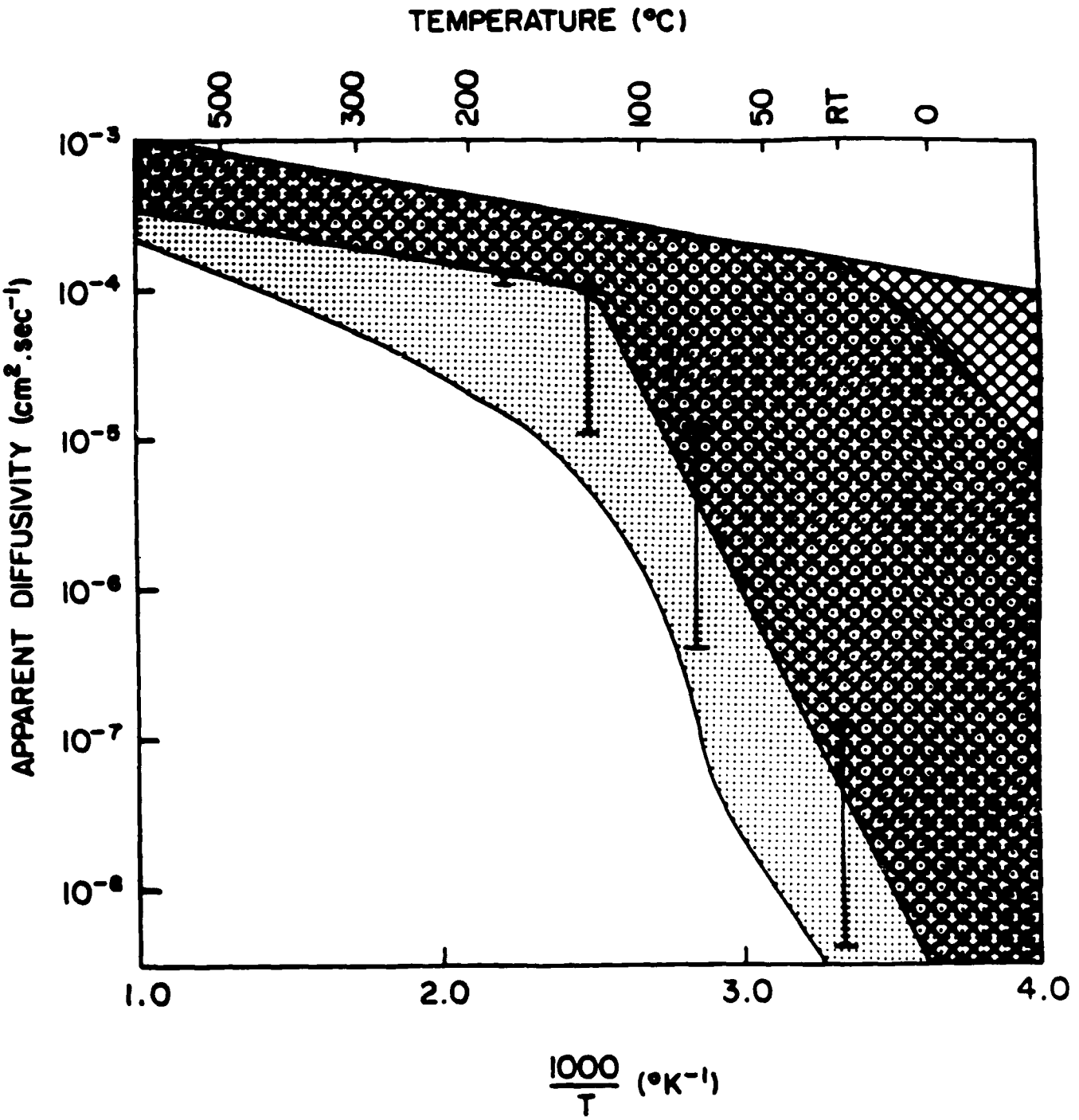
TEMPERATURE (°C)
500
300
200
100
50
RT
0
10^{-3}
10^{-4}
10^{-5}
10^{-6}
10^{-7}
10^{-8}
APPARENT DIFFUSIVITY ($cm^2.sec^{-1}$)
1.0
2.0
3.0
4.0
$\frac{1000}{T}$ ($°K^{-1}$)

Fig. 7

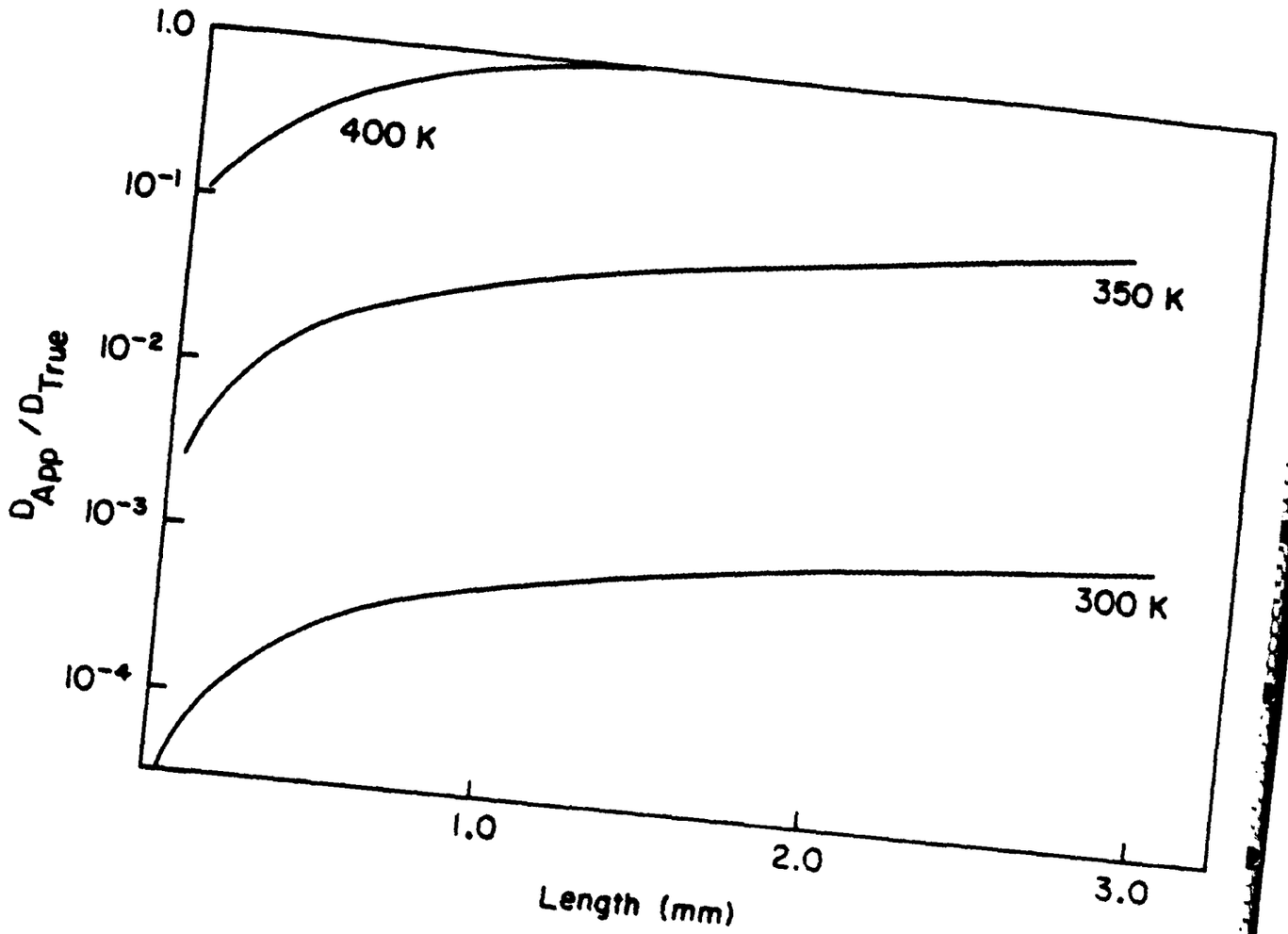
1.0
400 K
10^{-1}
350 K
10^{-2}
D_{App}/D_{True}
10^{-3}
300 K
10^{-4}
1.0
2.0
3.0
Length (mm)

END

9-87

DTIC